

# Towards an integrated framework for evidencing demographic buffering in natural populations

A manuscript in preparation for submission to ECOLOGY LETTERS

Type of article: METHOD

Gabriel Silva Santos<sup>1,2\*</sup>, Samuel J L Gascoigne<sup>3\*</sup>, André Tavares Corrêa Dias<sup>4</sup>, Maja Kajin<sup>3,5\*\*</sup> ♦, Roberto Salguero-Gómez<sup>3</sup> ♦

<sup>1</sup> National Institute of the Atlantic Forest (INMA), 29650-000, Santa Teresa, Espírito Santo, Brazil. ssantos.gabriel@gmail.com

<sup>2</sup> Department of Ecology, Graduate Program in Ecology and Evolution, Rio de Janeiro State University, 524 São Francisco Xavier Street, 20550-900, Maracanã, Rio de Janeiro, Brazil.

<sup>3</sup> Department of Biology, University of Oxford, South Parks Road, OX1 3RB, Oxford, UK. samuel.gascoigne@pmb.ox.ac.uk, rob.salguero@biology.ox.ac.uk

<sup>4</sup> Department of Ecology, Institute of Biology, Universidade Federal do Rio de Janeiro, Avenida Carlos Chagas Filho 373, 21941-590 Rio de Janeiro, RJ, Brazil. atcdias@gmail.com

<sup>5</sup> Chair of Zoology, Department of Biology, Biotechnical Faculty, University of Ljubljana, Večna pot 111, 1000 Ljubljana, Slovenia. maja.kajin@bf.uni-lj.si

\*Shared first authorship

\*\*Corresponding author

♦ Shared senior authorship

**AUTHOR CONTRIBUTIONS:** GSS developed the initial concept, performed the statistical analyses, and contributed to the first draft of the manuscript. SJLG developed the initial concept, contributed to the first draft and all other versions of the manuscript, and generated final figures. ATCD co-advised the project and contributed significantly to final versions of the manuscript. MK developed and managed the project, contributed to the first draft and all other versions of the manuscript, and generated final figures. RSG developed and managed the project and contributed to the first draft and all other versions of the manuscript. All authors made substantial contributions to editing the manuscript and further refining ideas and interpretations.

**RUNNING TITLE:** Demographic buffering framework (32/45 characters)

**KEYWORDS:** COMADRE Animal Matrix Database, elasticity, life-history evolution, natural selection, second-order derivative, sensitivity, stochasticity, variance.

**NUMBER OF WORDS:** Abstract – 146/150 words, main text (excluding abstract, acknowledgements, references, table, and figure legends) – 4979/5000 words

**NUMBER OF REFERENCES:** 86

**NUMBER OF TABLES:** 2 (in Supplementary Material)

**NUMBER OF FIGURES:** 3

**Abstract** (146/150 words)

The demographic buffering hypothesis predicts that natural selection reduces the temporal fluctuations in demographic processes (survival, development, and reproduction) due to their negative impacts of temporal variation on population dynamics. However, evidencing buffering patterns at different hierarchical levels – between and within populations – and understanding how selection shapes those patterns, remains a challenge in Ecology and Evolution. Here, we introduce a framework that allows for the evidencing of demographic buffering between and within populations. The framework uses the sum of stochastic elasticities for between-populations comparisons along with first- and second-order effects of demographic process variability on fitness for within-population comparisons. We apply this framework to 43 populations of 37 mammal species to test the hypothesis that buffered species are under strong concave selection pressures. Using our framework, we show that demographically buffered species do not necessarily have strong concave selection pressures in their most impactful demographic processes.

Environmental stochasticity shapes organisms' life histories (Bonsall & Klug 2011; Stearns 1992; Tuljapurkar 1990, 2010). Nonetheless, how organisms will cope with the changing variation in environmental conditions (Bathiany *et al.* 2018; Boyce *et al.* 2006; Morris *et al.* 2008) remains an intriguing ecological and evolutionary question (Sutherland *et al.* 2013). Evolutionary demography provides diverse explanations for how evolutionary processes shape demographic responses to environmental stochasticity (Charlesworth 1994; Healy *et al.* 2019; Hilde *et al.* 2020; Pfister 1998; Tuljapurkar *et al.* 2009). The long-term stochastic population growth rate ( $\lambda_s$ ) representing the geometric mean of population growth rates over time ( $\lambda_t$ ; Tuljapurkar 1982), forms the basis of the Demographic Buffering Hypothesis (Morris & Doak 2004; Pélabon *et al.* 2020).

Increasing the geometric mean of  $\lambda_t$  over time corresponds to a rise in the long-term stochastic population growth rate. Conversely, higher variance in  $\lambda_t$  reduces  $\lambda_s$  (Morris & Doak 2004; Tuljapurkar 1982), impacting population persistence (Lefèvre *et al.* 2016). The demographic buffering hypothesis (Pfister 1998) suggests life histories are selected to minimize the negative impacts of environmental variation by constraining the temporal variance of key demographic processes (*e.g.*, survival, development, reproduction) that have the highest sensitivity/elasticity to population growth rate, a fitness proxy (Gaillard & Yoccoz 2003; Pfister 1998). Demographic buffering describes the selection-driven constraint on the temporal variance of these key demographic processes (Gascoigne *et al.* 2024a, b; Hilde *et al.* 2020; Morris & Doak 2004; Pfister 1998). Here, we focus on the emerging patterns of demographic buffering in different animal life histories rather than on the demographic buffering hypothesis itself.

An integrative approach to evidence demographic buffering is still missing. Indeed, identifying demographic buffering remains challenging (Doak *et al.* 2005; Morris & Doak 2004) for several reasons, one of them being different interpretations of results from

correlational analyses, as in Pfister (1998) and Hilde *et al.* (2020). Some authors rank species' life histories on a continuum from buffered to labile using the correlation coefficient (Spearman's correlation  $\rho$ ) between the impact of demographic processes on the population growth rate and the temporal variance of said demographic processes (McDonald *et al.* 2017; Salguero-Gómez 2021). There, negative correlation coefficient values indicate buffering. Alternatively, the absence of statistical support for buffering may suggest a preference for demographic variance to track environmental conditions, a phenomenon supported by the Demographic Lability Hypothesis (Drake 2005; Hilde *et al.* 2020; Jäkäläniemi *et al.* 2013; Koons *et al.* 2009; Reed & Slade 2012). However, increased variability alone is not enough to constitute demographic lability; it must also result in significant changes in the mean value of the demographic process (Le Coeur *et al.* 2022).

Another obstacle to generalising a measure of demographic buffering across populations and species is the targeted hierarchical level of examination. Some studies focus on characteristics drawn from the *entire population model* (McDonald *et al.* 2017; Reed & Slade 2012). At this *between-populations level* (hereafter), a life history is considered demographically buffered if the governing demographic processes have low temporal variance (Le Coeur *et al.* 2022; Hilde *et al.* 2020; Morris & Doak 2004; Pfister 1998). However, to fully grasp how and why demographic buffering occurs, and how patterns might change in response to the environment, we must also consider characteristics within an individual population model (*within-populations level* hereafter). Within a population, one demographic process may be buffered against climatic variability while another may be labile (Barraquand & Yoccoz 2013; Jongejans *et al.* 2010; Koons *et al.* 2009). Furthermore, even if a given demographic process is primarily governing the population growth rate in one year, a different one might take over next year (Evers *et al.* 2021). Despite the relevance of within- and between-populations level processes, thus far studies have focused on evidencing

demographic buffering at the within- and between-population levels separately. To integrate these two levels of analysis, here we investigate demographic buffering signatures together.

To examine demographic buffering at the between-populations level, we use the *summed* effect of the variability of all demographic processes on the population growth rate. A weak summed effect means that the population growth rate is relatively unaffected by the variability in demographic processes (Haridas & Tuljapurkar 2005), and this lack of effect by demographic process variability is consistent with demographic buffering. As such, a summed effect of variability offers a good proxy to evidence demographic buffering (Gascoigne *et al.* 2024b; Haridas & Tuljapurkar 2005) and enables the classification of populations along a continuum. The within-populations level requires a separate approach. Thus, there we use the relative contribution of each demographic process and how variability in the governing demographic process(es) affects the population growth rate (*e.g.*, Caswell 1978, 1996, 2001; Ebert 1999; de Kroon *et al.* 1986). Importantly, by exploring the governing demographic processes, we also investigate how natural selection affects them (*e.g.*, Caswell 1996; Shyu & Caswell 2014). Understanding the interplay between demographic variability and natural selection thus not only elucidates population dynamics but also provides insight into the evolutionary pressures shaping the life-history strategies (Charlesworth 1994; Salguero-Gómez 2024; Sanghvi *et al.* 2024).

A powerful approach to reveal the role of natural selection acting on the variability of demographic processes is through measuring a first and second order effect on population growth rate (Carslake *et al.* 2008). First-order effects of demographic processes on population growth rate, such as elasticities, show how *variation* in demographic processes affects population growth rate, and relies on the *linear* relation between demographic processes and the growth rate. A second-order effect, on the other hand, reveals the sensitivity of population growth rate to temporal *autocorrelation* in variable environments (Tuljapurkar 1990), and

identifies where demographic processes have a *nonlinear* effect on population growth rate. Combining both approaches into a single framework consolidates our understanding of fitness behaviour near local maxima and minima, among other advantages discussed below. This approach and has started to pave its way into Ecology (Kajin *et al.* 2023; Tuljapurkar *et al.* 2023).

Here, we propose that an additional metric to examine demographic buffering: the second-order effect of demographic process variation on population growth rate. We show that each hierarchical level is best studied with a different method. Moreover, we hypothesise that buffered species, those where perturbing the variance of demographic processes has little impact on their fitness, are under strong concave selection pressures (*i.e.*, the force that aims to diminish temporal variance of a trait, sensu Shyu & Caswell 2014) on the governing demographic processes. Indeed, the summed effect of demographic process variability on population growth rate and elasticities are related (Haridas & Tuljapurkar 2005). Concave selection pressures favour traits that contribute to reducing temporal variance, thereby enhancing population stability and resilience in the face of environmental volatility. We discuss the validity of our hypothesis and demonstrate the applicability and advantages of our framework by testing it with 43 populations of 37 mammal species.

## **Towards an integrated framework to assess evidence of demographic buffering**

Current evidence for demographic buffering has primarily been assessed using Matrix Population Models (*MPMs*) (Pfister 1998; Rotella *et al.* 2012). However, Integral Projection Models (*IPMs*) (Easterling *et al.* 2000; Ellner *et al.* 2016; Gascoigne *et al.* 2023a, 2024b; Rodríguez-Caro *et al.* 2021; Wang *et al.* 2023) can also identify demographic buffering. *MPMs* and *IPMs* are structured, discrete-time demographic models (Caswell 2001; Ellner *et al.* 2016). For simplicity, here we focus on *MPMs*, but the same approaches apply to *IPMs*

(Doak *et al.* 2021; Griffith 2017). We refer to demographic processes as MPM  $A$  entries  $a_{ij}$  (*i.e.*, upper-level parameters *sensu* Zuidema & Franco 2001) and the vital rates composing the matrix elements (*i.e.*, lower-level parameters, *ditto*). The conversion between matrix elements and vital rates is straightforward (Franco & Silvertown 2004).

We first place species on a variance continuum. The variance continuum represents the *summed* effects of proportional increases in temporal variance across all demographic processes ( $a_{ij}$ ) of the MPM  $A$  on the population growth rate  $\lambda_s$ , operating at the *between-populations level*. It is based on partitioning the sum of all the stochastic elasticities ( $\Sigma E_{a_{ij}}^S$ ) into two components: i) the sum of stochastic elasticities with respect to the variance ( $\Sigma E_{a_{ij}}^{S^\sigma}$ ), which assesses how variability in  $a_{ij}$  affects  $\lambda_s$ , and ii) the sum of stochastic elasticities with respect to the arithmetic mean of demographic processes ( $\Sigma E_{a_{ij}}^{S^\mu}$ ), which evaluates the impact of a change in mean values of demographic processes on  $\lambda_s$  (Haridas & Tuljapurkar 2005).

The equal perturbation of both  $\Sigma E_{a_{ij}}^S$  components assumes that the CV of demographic processes remains constant (Haridas & Tuljapurkar 2005). Higher absolute value of  $\Sigma E_{a_{ij}}^{S^\sigma}$  indicates greater sensitivity of  $\lambda_s$  to demographic process variability, suggesting the absence of demographic buffering. Conversely, lower  $\Sigma E_{a_{ij}}^{S^\sigma}$  values support the demographic buffering hypothesis, with  $\lambda_s$  being less sensitive to variability (Haridas & Tuljapurkar 2005; Tuljapurkar *et al.* 2003) (Fig. 1A).

Species or populations are positioned along the variance continuum based on the impact of variance on the stochastic population growth rate. Species highly sensitive to environmental variability are on the left (potentially unbuffered<sup>1</sup>), while species less sensitive

---

<sup>1</sup> Unconstrained variance does not necessarily imply demographic lability, defined as an increase in *mean value* of a demographic process in response to improved environmental conditions (Le Coeur *et al.* 2022). By examining stochastic elasticities, we can assess changes in the contribution of demographic process variance to  $\lambda_s$ , while mean values remain unchanged.

are on the right (potentially buffered) end (Fig. 1A). We expect buffered species to exhibit concave selection signatures. Although the position on the continuum provides insight into how environmental variation affects  $\lambda_s$ ,  $\Sigma E_{a_{ij}}^{S\sigma}$  does not consider covariances between demographic processes and serial correlations, crucial for fully diagnosing buffering (Haridas & Tuljapurkar 2005). Thus, species' position at the buffered end of the variance continuum is a *necessary but not sufficient* condition for evidence of demographic buffering. To address this second criterion, we use second derivatives of population growth rate with respect to demographic processes to elucidate the impact of selection on variance (below).

Next, we delve into within-population level by calculating the partial derivatives of  $\lambda_l$  (obtained by averaging sequential MPMs across the study duration) concerning all matrix elements  $a_{ij}$  of the MPM  $A$  (Fig. 1B). This step reveals a first-order effect on fitness — how each demographic process influences  $\lambda_l$ . We then evaluate nonlinear selection patterns using self-second derivatives of  $\lambda_l$  for each  $a_{ij}$  (Fig. 1C), revealing potential nonlinear selection pressures (Brodie *et al.* 1995). Failure to consider these evolutionary processes may lead to misinterpretation of patterns (*e.g.*, Lawler *et al.* 2009).

First- and second-order effects on fitness show average selection pressures over time. Self-second derivatives of population growth rate with respect to demographic processes measure second-order effects (Carslake *et al.* 2008; Caswell 2001; Kajin *et al.* 2023; Shyu & Caswell 2014; Tuljapurkar *et al.* 2023). Linear fitness relationships (zero self-second derivatives) mean selection changes mean demographic values, not variance (Shyu & Caswell 2014). Nonzero self-second derivatives indicate nonlinear relationships between fitness and a demographic process, revealing additional aspects of selection on the variances and covariances of demographic processes (Brodie *et al.* 1995; Carslake *et al.* 2008; Shyu & Caswell 2014). Interpreting both first- and second-order effects offers insights into population placement on the variance continuum.



The sign ( $>0$ ,  $=0$ ,  $<0$ ) of the self-second derivatives determines the selection type. Negative values (concave selection,  $\cap$ -shaped) reduce temporal variance, providing evidence of buffering (Caswell 1996, 2001; Shyu & Caswell 2014). Positive values (convex selection, U-shaped) indicate amplified variance, revealing a lack of selection constraints on demographic variance (Bruijning *et al.* 2020; Caswell 1996, 2001; Le Coeur *et al.* 2022; Koons *et al.* 2009; Shyu & Caswell 2014; Vinton *et al.* 2022).

Following the above steps allows evidencing demographic buffering at the between- and within-populations levels. The joint interpretation of first- and second-order effects offers insights into why a population is on either end of the variance continuum. Evidence supporting buffering includes:

1. A population positioned near the 0 end of the  $\Sigma E_{a_{ij}}^{S^\sigma}$  continuum.
2. Identifying the demographic processes with highest elasticity values within the life cycle.
3. The same processes from (2) associated with negative self-second derivatives, indicating concave selection.

Figure 1B shows that, for an imaginary wolf population, the governing demographic process is the fourth stage stasis (MPM element  $a_{4,4}$ ), with the highest elasticity value (Fig. 1B yellow square). However, Figure 1C reveals little selection on  $a_{4,4}$  for variance reduction. Hence, there is no concave selection on  $a_{4,4}$ , explaining the positioning on the left-side variance continuum (Fig. 1A).

Although not our primary goal, we briefly introduce steps to evidence demographic lability. Compelling lability evidence requires sufficient data across environments [over time or space; but see Perret *et al.* (2024)] to construct reaction norms depicting demographic responses to environmental changes (Drake 2005; Koons *et al.* 2009; Morris *et al.* 2008). Non-linear relationships between demographic processes and the environment must be

established based on the reaction norms. Demographic processes where an increase in the mean value has a stronger positive impact on population growth rate than the detrimental effect of increased variance need to be identified. The latter condition is only met when the process-environment reaction norms are convex (Drake 2005, Koons *et al.* 2009, Morris *et al.* 2008) – but see Barraquand & Yoccoz (2013) for an alternative result. Importantly, species may not be purely buffered or labile some processes may be buffered, others labile, and others insensitive to environmental variability (*e.g.*, Doak *et al.* 2005). Deciphering these patterns is a primary research interest in the field.

#### **Demographic buffering in mammals: A case study**

Here, we examine the performance of our framework and test our hypothesis, that is that species at the buffered end of the variance continuum display highly negative self-second derivatives for the governing demographic processes. We use 43 MPMs from 37 mammal species (16 species at the within-populations level). Mammals are of special interest in the context of demographic buffering for two reasons: (1) mammalian life histories have been well studied (Beccari *et al.* 2024; Bielby *et al.* 2007; Gillespie 1977; Jones 2011; Stearns 1983) and (2) some of their populations have already been assessed in terms of demographic buffering, particularly for primates (Campos *et al.* 2017; Morris *et al.* 2008, 2011; Reed & Slade 2012; Rotella *et al.* 2012). Together, the well-studied life histories and previous information about the occurrence of buffering in mammals allow us to make accurate predictions and validate the performance of our framework.

We used MPMs (Caswell 2001) from 43 out of 139 studies with mammals available in the COMADRE Animal Matrix Database v.3.0.0 (Salguero-Gómez *et al.* 2016). These 43 populations encompass 37 species from eight taxonomic orders. We carefully selected these MPMs in our analyses because their models contain values of demographic processes ( $a_{ij}$ )

for three or more contiguous time periods, thus allowing us to obtain the stochastic elasticity of each  $a_{ij}$ . Although we are aware that not all possible temporal variation in demographic processes may have been expressed within this period, we assumed three or more transitions are enough to provide sufficient variation for population comparison (Compagnoni *et al.* 2023). To mitigate bias in variance estimates, we randomly extracted three MPMs from the existing data for each species (Supplementary Material, Table S1), calculated the mean of these three MPMs, and repeated this process 50 times to obtain estimates of  $\Sigma E_{a_{ij}}^{S\sigma}$  and their corresponding standard errors. A detailed description of the analysed data and their original sources are detailed in Table S1. Finally, we included MPMs of *Homo sapiens* to cross-check our estimates of second-order derivatives, as it is the only mammalian species where these have been calculated (Caswell 1996). The data for *H. sapiens* were gathered from 26 modern populations (Keyfitz & Flieger 1990).

At the within-populations level, we used a subset of 16 populations (including *H. sapiens*) whose MPMs were age-based. We specifically selected these populations because their life cycles can be summarised by two main demographic processes: survival and contribution to the recruitment of new individuals (Caswell 2010; Ebert 1999).

To quantify the variance continuum and calculate  $\Sigma E_{a_{ij}}^{S\sigma}$  for between-populations level comparisons, we followed Tuljapurkar *et al.* (2003) and Haridas & Tuljapurkar (2005). Next, at the within-populations level, we calculated the deterministic elasticities to each demographic process using the *popbio* package (Stubben *et al.* 2020). The self-second derivatives were adapted from *demogR* (Jones 2007) following (Caswell 1996) and applied to the mean MPM of each study. All analyses were performed using R version 4.4.1 (R Core Team 2024).

## Results

286 We ranked 43 populations from the 37 identified mammal species into a variance continuum  
 287 according to the cumulative impact of variation in demographic processes on  $\lambda_s$  (Fig. 2). Most  
 288 of the analysed taxonomic orders were placed on the low or zero variance end of the variance  
 289 continuum (Fig. 2), corroborating with demographically buffered populations. The smallest  
 290 contributions of variation in demographic processes (note that  $\Sigma E_{a_{ij}}^{S^\sigma}$  ranges from 0 to -1),  
 291 suggesting buffered populations, were assigned to Primates: northern muriqui (*Brachyteles*  
 292 *hyphoxantus*,  $\Sigma E_{a_{ij}}^{S^\sigma} = -5.31 \times 10^{-5} \pm 2.09 \times 10^{-5}$ ) (mean  $\pm$  S.E.) (Fig. 2 silhouette a), mountain  
 293 gorilla (*Gorilla beringei*,  $\Sigma E_{a_{ij}}^{S^\sigma} = -1.28 \times 10^{-5} \pm 1.32 \times 10^{-5}$ ) (Fig. 2 silhouette b), followed by  
 294 the blue monkey (*Cercopithecus mitis*,  $\Sigma E_{a_{ij}}^{S^\sigma} = -4.43 \times 10^{-5} \pm 1.18 \times 10^{-5}$ ) (Fig. 2 silhouette  
 295 c). The first non-primate species placed near the buffered end of the continuum was the  
 296 Columbian ground squirrel (*Urocitellus columbianus*, Rodentia,  $\Sigma E_{a_{ij}}^{S^\sigma} = -3.38 \times 10^{-3} \pm 6.96 \times$   
 297  $10^{-4}$ ) (Fig. 2 silhouette d). On the other opposite, the species with the highest contribution of  
 298 variation in demographic processes – placed at the high-variance end of the continuum –  
 299 was the stoat (*Mustela erminea*, Carnivora,  $\Sigma E_{a_{ij}}^{S^\sigma} = -0.310 \pm 0.0162$ ) (Fig. 2 silhouette e). All  
 300 the 14 primate populations occupied the buffered side of the variance continuum, with the  
 301 exception of the Patas monkey (*Erythrocebus patas*, Primates,  $\Sigma E_{a_{ij}}^{S^\sigma} = -0.0521 \pm 5.38 \times 10^{-3}$ )  
 302 (Fig. 2 silhouette f). The snowshoe hare (*Lepus americanus*, Lagomorpha,  $\Sigma E_{a_{ij}}^{S^\sigma} = -0.262 \pm$   
 303  $0.0233$ ) (Fig. 2 silhouette g) and the Bush rat (*Rattus fuscipes*, Rodentia,  $\Sigma E_{a_{ij}}^{S^\sigma} = -0.245 \pm$   
 304  $4.29 \times 10^{-3}$ ) (Fig. 2 silhouette h) were positioned on the non-buffered end of the variance  
 305 continuum. Additional information (including standard errors of the elasticity estimates) is  
 306 provided in Table S1. *A posteriori*, we quantified the impact of phylogenetic relatedness on  
 307 the estimates of the sum of stochastic elasticities (Fig. 2), and then for the correlation  
 308 between those estimates and the number of MPMs available per species. For the former, we  
 309 estimated Blomberg's K, a measure of phylogenetic signal that ranges between 0 (weak

signal) to positive values 1 (strong) (Münkemüller *et al.* 2012). Blomberg's K in our analyses was 0.23. The correlation between the number of available MPMs per study and the sum of stochastic elasticities (post jack-knifing) raised a weakly negative coefficient (-0.002), though significant ( $P = 0.017$ ).

We found little evidence in support of our hypothesis. Specifically, the demographic processes with the highest elasticity values failed to display strong negative self-second derivatives (Fig. 3). Particularly for the majority of primates, demographic processes with high elasticities had positive values for the self-second derivatives (indicated by yellow squares with white dots in Figure 3). Examples of primate species exhibiting high elasticities and positive values for their self-second derivatives include northern muriqui (*Brachyteles hypoxanthus*), mountain gorilla (*Gorilla beringei*), white-faced capuchin monkey (*Cebus capucinus*), rhesus monkey (*Macaca mulatta*), blue monkey (*Cercopithecus mitis*), Verreaux's sifaka (*Propithecus verreauxi*) and olive baboon (*Papio cynocephalus*) (Fig. 3). This implies that the key demographic processes influencing  $\lambda_1$  do not show evidence of selective pressure for reducing their variability.

The killer whale (*Orcinus orca*) showed similar lack of support for our hypothesis as primates. Indeed, *O. orca* was positioned at the buffered end of the variance continuum (Cetacea,  $\Sigma E_{a_{ij}}^{S\sigma} = -4.72 \times 10^{-4} \pm 1.53 \times 10^{-4}$ ) (Fig. 2 silhouette not shown). However, the first- and second-order effects show that the governing three demographic processes in the killer whale life cycle (namely, matrix elements  $a_{2,2}$ ,  $a_{3,3}$ , and  $a_{4,4}$ ) are not under selection pressures for reducing their temporal variance, but the opposite (yellow and green squares with white dots, Fig. 3).

Only two species supported our hypothesis: humans and the Columbian ground squirrel (*Urocitellus columbianus*). In humans, demographic parameters representing survival from the first to second age class (matrix element  $a_{2,1}$ ) displayed high elasticities and negative

self-second derivatives (depicted as yellow squares with black dots in Fig. 3). In *U. columbianus*, survival from the first to the second age class ( $a_{2,1}$ ) too showed evidence of selection reducing the variance of this demographic process. Accordingly, *U. columbianus* was positioned near the buffered end of the variance continuum, providing consistent evidence supporting our hypothesis by displaying first- and second-order effects indicative of temporal variance reduction in the key demographic process. Conversely, the primary governing demographic process for Soay sheep (*Ovis aries*) displayed convex selection signatures. For *O. aries* (Fig. 2, silhouette i), remaining in the third age class ( $a_{3,3}$ , Fig. 3) governs the influence on  $\lambda_t$  and is under selection pressure to have its variance increased. These characteristics suggest potential conditions for lability, despite the species being positioned closer to the buffered end of the variance continuum.

The first- and second-order effects illustrate the importance of examining buffering evidence at the within-populations level. These effects can identify the simultaneous contributions of concave and convex selection on different demographic processes within a single life cycle. In the polar bear (*Ursus maritimus*), the key demographic process ( $a_{4,4}$ ) is under convex selection, as depicted by a yellow square with a white dot in Figure 3. However, the demographic process with the second highest elasticity value ( $a_{5,4}$ ) is under strong concave selection (depicted by a light green square with a black dot in Figure. 3).

By adding the second-order effect to the toolbox for demographic buffering, another important inference was made possible. The high absolute values of self-second derivatives (large dots, either black or white, Fig. 3) indicate where the sensitivity of  $\lambda_t$  to demographic parameters is itself prone to environmental changes. For instance, if the value of  $a_{5,4}$  for *U. maritimus* increased, the sensitivity of  $\lambda_t$  to  $a_{5,4}$  would decrease because the self-second derivative of  $a_{5,4}$  is highly negative (depicted by the largest black dot in polar bear, Fig. 3 silhouette j). The opposite holds for the  $a_{4,4}$  demographic process, where an increase in the

value of  $a_{4,4}$  would increase the sensitivity of  $\lambda_t$  to  $a_{4,4}$ , because the self-second derivative of  $a_{4,4}$  is highly positive (the largest white dot in the polar bear MPM). Thus, sensitivities (or equally elasticities) of demographic processes with high absolute values for self-second derivatives are dynamic and can easily change.

## Discussion

We report evidence of demographic buffering assessed at the between and within populations level. We used stochastic elasticities alongside the first- and second- order perturbation analysis and applied these analyses to mammal species to test our hypothesis. Here, we find weak support for said hypothesis, since most populations placed at the buffered end of variance continuum failed to display concave selection signatures.

Evidencing demographic buffering is not straightforward. Indeed, through the analysis of stochastic population growth rate ( $\lambda_s$ ) in our application of the framework to 43 populations of 37 mammal species, we identify the highest density of natural populations near the buffered end of the variance continuum. However, we show that the same species then fail to exhibit signs of concave ( $\cap$ -shaped) selection on key demographic parameters, opposed to our hypothesis. Such results suggest discordance between two features of demographic buffering, namely: 1) the stochastic population growth rate having a low sensitivity to temporal variability in demographic processes, and 2) demographic processes having variability constrained by selection.

The lack of correlation between non-linear selection patterns (concave/convex) and species positioning on the variance continuum for the studied mammal species may have several explanations. Firstly, non-linear selection on demographic process variability is *dynamic* (Kajin *et al.* 2023). Within a life cycle, even minor changes in key demographic processes can trigger a domino effect, affecting not only the process itself but also the

sensitivity of  $\lambda_1$  to changes in said process (Stearns 1992). Consequently, correlations between demographic processes (negative correlations known as trade-offs) are influenced by minor alterations in the governing demographic processes (Doak *et al.* 2005). Therefore, the observed self-second derivative of the population growth rate represents a momentum that can be influenced by small changes in any demographic process within the life cycle. Because of these characteristics, second-order derivatives reveal “fine scale” fitness behaviour compared to sums of stochastic elasticities. Evolutionary demography still requires a tool to connect second-order fitness effects with stochastic elasticities in a biologically interpretable manner (but see Tuljapurkar *et al.* 2023).

When placing our study species along a variance continuum, primates tend to be located on the buffered end. However, most primates displayed convex – instead of the expected concave – selection on adult survival. Similar results, where the key demographic process failed to display constrained temporal variability, have been reported for long-lived seabirds (Doherty *et al.* 2004). One explanation for the unexpected convex selection on adult survival involves trade-offs, as suggested by (Doak *et al.* 2005). When two demographic parameters are negatively correlated, the variance of population growth rate can be increased or decreased (Compagnoni *et al.* 2016; Evans & Holsinger 2012).

Correlations among demographic processes (positive and negative) inherently influence the biological limits of variance (Haridas & Tuljapurkar 2005). This is because the magnitude of variation in a particular demographic process is constrained by the variation of other demographic processes. Not surprisingly, correlations among demographic processes have been shown to be strongly subjected to ecological factors (Fay *et al.* 2022). Therefore, future studies may benefit from deeper insights using *cross*-second derivatives (Caswell 1996, 2001) to investigate correlations among demographic processes.



Biological variance estimates are inevitably subjected to several sources of bias (Simmonds & Jones 2024). To minimise bias, we randomly sampled the available matrices before obtaining the estimates. Despite the significant correlation between  $\Sigma E_{a_{ij}}^{S\sigma}$  and the number of available matrices per species, the relative positioning of species remains meaningful for between-population level comparisons, as the correlation is very weak (-0.002). Still, researchers carrying out macroecological comparisons of demographic buffering might want to be even more stringent than we have been here with their datasets, as these grow longer with time (Compagnoni *et al.* 2021; Salguero-Gómez *et al.* 2021).

Regarding phylogenetic effects, our tests revealed a mild signal, but we note that future work regressing  $\Sigma E_{a_{ij}}^{S\sigma}$  values against potential independent variables (*e.g.*, climate values) may want to correct for this phylogenetic dependence. By having carefully chosen studies from a database that contains >400 species and retained only those that passed through a set of selection criteria (Che-Castaldo *et al.* 2020; Gascoigne *et al.* 2023b; Kendall *et al.* 2019; Römer *et al.* 2024; Simmonds & Jones 2024), we mitigate those biases *a priori*. Furthermore, we are using an elasticity-based approach, meaning we are comparing proportional variances. At present, the available methods still do not account for constraints in variance nor performing a perturbation approach disproportionately.

The analyses at both between- and within-populations levels are fundamentally interconnected. This connection is grounded on the fact that large summed elasticities with respect to variance are intrinsically linked to high elasticity values, as demonstrated in equation 6 in (Haridas & Tuljapurkar 2005). This finding robustly endorses the perspective that species' positions along the variance continuum should be interpreted with consideration of first and second-order effects, and additionally, in the context of selection pressures acting on the variability of demographic processes, as revealed by a second order effect.

Combining first- and second-order analyses is crucial for understanding the factors shaping demographic buffering patterns. The second-order effect reveals that the role of natural selection in shaping temporal variation in demographic processes is more complex than initially thought. Indeed, demographic processes within our study populations often face a mix of convex and concave selection. This mix of selection patterns was suggested by Doak et al. (2005), who noted that dramatic changes in population growth rate sensitivities are influenced by correlations among demographic processes. Here, only two of the 16 mammal species revealed concave selection on the key demographic processes: Columbian ground squirrel (*Urocitellus columbianus*), and humans (*Homo sapiens*). These two species were placed near the buffered end of the variance continuum, supporting our hypothesis. Evidence of buffering has been reported across 22 ungulate species (Gaillard & Yoccoz 2003). However, in the one ungulate we examined, the moose (*Alces alces*), we found only partial support for our hypothesis, as it is near the buffered end of the variance continuum but lacks concave selection pressures.

Our overall findings reveal varying levels of support for the notion that adult survival in long-lived species tends to be buffered. Indeed, Gaillard et al. (1998) found that adult female survival varied considerably less than juvenile survival in large herbivores. This finding was also supported by further studies in ungulates (Gaillard & Yoccoz 2003), turtles (Heppell 1998), vertebrates and plants (Pfister 1998), and more recently across nine species of plants (McDonald et al. 2017). However, an alternative result was also reported by Gaillard and Yoccoz (2003) for small mammals, where variability in adult survival was unexpectedly high, even though the studied small mammals were annual, and as such comparable to large mammal model. Seasonality, frequency and method of sampling all influence survival estimates and their estimated variability, thus, when comparing multiples

species/studies, all of the latter characteristics should be taken into account when interpreting the results.

Examining the drivers of demographic buffering has become an important piece of the ecological and evolutionary puzzle of demography. As such, understanding buffering can help us better predict population responses to environmental variability, climate change, and direct anthropogenic disturbances (Boyce *et al.* 2006; Gascoigne *et al.* 2024a; McDonald *et al.* 2017; Pfister 1998; Vázquez *et al.* 2017). By setting demographic buffering into a broader and integrated framework, we hope to enhance comprehension and prediction of the implications of heightened environmental stochasticity on the evolution of life history traits. This understanding is crucial in mitigating the risk of extinction for the most vulnerable species.

## Acknowledgements

This study was financed in part by the *Coordenação de Aperfeiçoamento de Pessoal de Nível Superior* - Brasil (CAPES) - Finance Code 001. GSS was supported by CAPES and CNPq (301343/2023-3). MK was supported by the European Commission through the Marie Skłodowska-Curie fellowship (MSCA MaxPersist #101032484) hosted by RSG. RS-G was supported by a NERC Independent Research Fellowship (NE/M018458/1) and a NERC Pushing the Frontiers (NE/X013766/1).

## Data availability

The demographic data used in this paper are open-access and available in the COMADRE Animal Matrix Database (<https://compadre-db.org/Data/Comadre>). A list of the studies and species used here is available in Supplementary Material (Table S1). The data and code

supporting the results can be accessed here:

[https://github.com/SamuelGascoigne/Demographic\\_buffering\\_unified\\_framework](https://github.com/SamuelGascoigne/Demographic_buffering_unified_framework).

## References

- Barraquand, F. & Yoccoz, N.G. (2013). When can environmental variability benefit population growth? Counterintuitive effects of nonlinearities in vital rates. *Theor Popul Biol*, 89, 1–11.
- Bathiany, S., Dakos, V., Scheffer, M. & Lenton, T.M. (2018). Climate models predict increasing temperature variability in poor countries. *Sci Adv*, 4.
- Beccari, E., Capdevila, P., Salguero-Gómez, R. & Carmona, C.P. (2024). Worldwide diversity in mammalian life histories: Environmental realms and evolutionary adaptations. *Ecol Lett*, 27.
- Bielby, J., Mace, G.M., Bininda-Emonds, O.R.P., Cardillo, M., Gittleman, J.L., Jones, K.E., *et al.* (2007). The Fast-Slow Continuum in Mammalian Life History: An Empirical Reevaluation. *Am Nat*, 169, 748–757.
- Bonsall, M.B. & Klug, H. (2011). The evolution of parental care in stochastic environments. *J Evol Biol*, 24, 645–655.
- Boyce, M., Haridas, C., Lee, C. & The NCEAS Stochastic Demography Working Group. (2006). Demography in an increasingly variable world. *Trends Ecol Evol*, 21, 141–148.
- Brodie, E.I., Moore, A. & Janzen, F. (1995). Visualizing and quantifying natural selection. *Trends Ecol Evol*, 10, 313–318.
- Campos, F.A., Morris, W.F., Alberts, S.C., Altmann, J., Brockman, D.K., Cords, M., *et al.* (2017). Does climate variability influence the demography of wild primates? Evidence from long-term life-history data in seven species. *Glob Chang Biol*, 23, 4907–4921.
- Carslake, D., Townley, S. & Hodgson, D.J. (2008). Nonlinearity in eigenvalue-perturbation curves of simulated population projection matrices. *Theor Popul Biol*, 73, 498–505.
- Caswell, H. (1978). A general formula for the sensitivity of population growth rate to changes in life history parameters. *Theor Popul Biol*, 14, 215–230.
- Caswell, H. (1996). Second Derivatives of Population Growth Rate: Calculation and Applications. *Ecology*, 77, 870–879.
- Caswell, H. (2001). *Matrix Population Models: Construction, Analysis, and Interpretation*. Sinauer Associates Inc. Publishers, Sunderland, Massachusetts, USA.
- Charlesworth, B. (1994). *Evolution in age-structured populations*. second edi. Cambridge University Press.
- Che-Castaldo, J., Jones, O.R., Kendall, B.E., Burns, J.H., Childs, D.Z., Ezard, T.H.G., *et al.* (2020). Comments to “Persistent problems in the construction of matrix population models.” *Ecol Modell*, 416.
- Le Coeur, C., Yoccoz, N.G., Salguero-Gómez, R. & Vindenes, Y. (2022). Life history adaptations to fluctuating environments: Combined effects of demographic buffering and lability. *Ecol Lett*, 25, 2107–2119.
- Compagnoni, A., Bibian, A.J., Ochocki, B.M., Rogers, H.S., Schultz, E.L., Sneek, M.E., *et al.* (2016). The effect of demographic correlations on the stochastic population dynamics of perennial plants. *Ecol Monogr*, 86, 480–494.
- Compagnoni, A., Evers, S. & Knight, T. (2023). Spatial replication can best advance our understanding of population responses to climate. *bioRxiv*, <https://doi.org/10.1101/2022.06.24.497542>.

527 Compagnoni, A., Levin, S., Childs, D.Z., Harpole, S., Paniw, M., Römer, G., *et al.* (2021).  
 528 Herbaceous perennial plants with short generation time have stronger responses to  
 529 climate anomalies than those with longer generation time. *Nat Commun*, 12, 1824.  
 530 Doak, D.F., Morris, W.F., Pfister, C., Kendall, B.E. & Bruna, E.M. (2005). Correctly  
 531 Estimating How Environmental Stochasticity Influences Fitness and Population Growth.  
 532 *Am Nat*, 166, E14–E21.  
 533 Doak, D.F., Waddle, E., Langendorf, R.E., Louthan, A.M., Isabelle Chardon, N., Dibner,  
 534 R.R., *et al.* (2021). A critical comparison of integral projection and matrix projection  
 535 models for demographic analysis. *Ecol Monogr*, 91, e01447.  
 536 Doherty, P.F., Schreiber, E.A., Nichols, J.D., Hines, J.E., Link, W.A., Schenk, G.A., *et al.*  
 537 (2004). Testing life history predictions in a long-lived seabird: A population matrix  
 538 approach with improved parameter estimation. *Oikos*, 105, 606–618.  
 539 Drake, J.M. (2005). Population effects of increased climate variation. *Proceedings of the*  
 540 *Royal Society B: Biological Sciences*, 272, 1823–1827.  
 541 Easterling, M.R., Ellner, S.P. & Dixon, P.M. (2000). Size-Specific Sensitivity: Applying a  
 542 New Structured Population Model. *Ecology*, 81, 694–708.  
 543 Ebert, T. (1999). *Plant and animal populations: Methods in demography*. Academic Press,  
 544 San Diego, CA, USA.  
 545 Ellner, S.P., Childs, D.Z. & Rees, M. (2016). *Data-driven Modelling of Structured*  
 546 *Populations. A practical guide to the Integral Projection Model*. Lecture Notes on  
 547 Mathematical Modelling in the Life Sciences. Springer International Publishing, Cham.  
 548 Evans, M.E.K. & Holsinger, K.E. (2012). Estimating covariation between vital rates : A  
 549 simulation study of connected vs . separate generalized linear mixed models (GLMMs).  
 550 *Theor Popul Biol*, 82, 299–306.  
 551 Evers, S.M., Knight, T.M., Inouye, D.W., Miller, T.E.X., Salguero-Gómez, R., Iler, A.M., *et*  
 552 *al.* (2021). Lagged and dormant season climate better predict plant vital rates than  
 553 climate during the growing season. *Glob Chang Biol*, 27, 1927–1941.  
 554 Fay, R., Hamel, S., van de Pol, M., Gaillard, J.M., Yoccoz, N.G., Acker, P., *et al.* (2022).  
 555 Temporal correlations among demographic parameters are ubiquitous but highly  
 556 variable across species. *Ecol Lett*, 25, 1640–1654.  
 557 Franco, M. & Silvertown, J. (2004). A comparative demography of plants based upon  
 558 elasticities of vital rates. *Ecology*, 85, 531–538.  
 559 Gaillard, J.M., Festa-Bianchet, M. & Yoccoz, N.G. (1998). Population dynamics of large  
 560 herbivores: Variable recruitment with constant adult survival. *Trends Ecol Evol*, 13, 58–  
 561 63.  
 562 Gaillard, J.-M. & Yoccoz, N. (2003). Temporal Variation in Survival of Mammals: a Case of  
 563 Environmental Canalization? *Ecology*, 84, 3294–3306.  
 564 Gascoigne, S.J.L., Kajin, M. & Salguero-Gómez, R. (2024a). Criteria for buffering in  
 565 ecological modeling. *Trends Ecol Evol*, 39, 116–118.  
 566 Gascoigne, S.J.L., Kajin, M., Sepil, I. & Salguero-Gómez, R. (2024b). Testing for efficacy in  
 567 four measures of demographic buffering. *EcoEvoRxiv*, 0–2.  
 568 Gascoigne, S.J.L., Kajin, M., Tuljapurkar, S.D., Silva Santos, G., Compagnoni, A., Steiner,  
 569 U.K., *et al.* (2023a). Structured demographic buffering: A framework to explore the  
 570 environment drivers and demographic mechanisms underlying demographic buffering.  
 571 *bioRxiv*.  
 572 Gascoigne, S.J.L., Rolph, S., Sankey, D., Nidadavolu, N., Stell Pičman, A.S., Hernández,  
 573 C.M., *et al.* (2023b). A standard protocol to report discrete stage-structured demographic  
 574 information. *Methods Ecol Evol*, 14, 2065–2083.  
 575 Gillespie, J.H. (1977). Natural Selection for Variances in Offspring Numbers: A New  
 576 Evolutionary Principle. *Am Nat*, 111, 1010–1014.

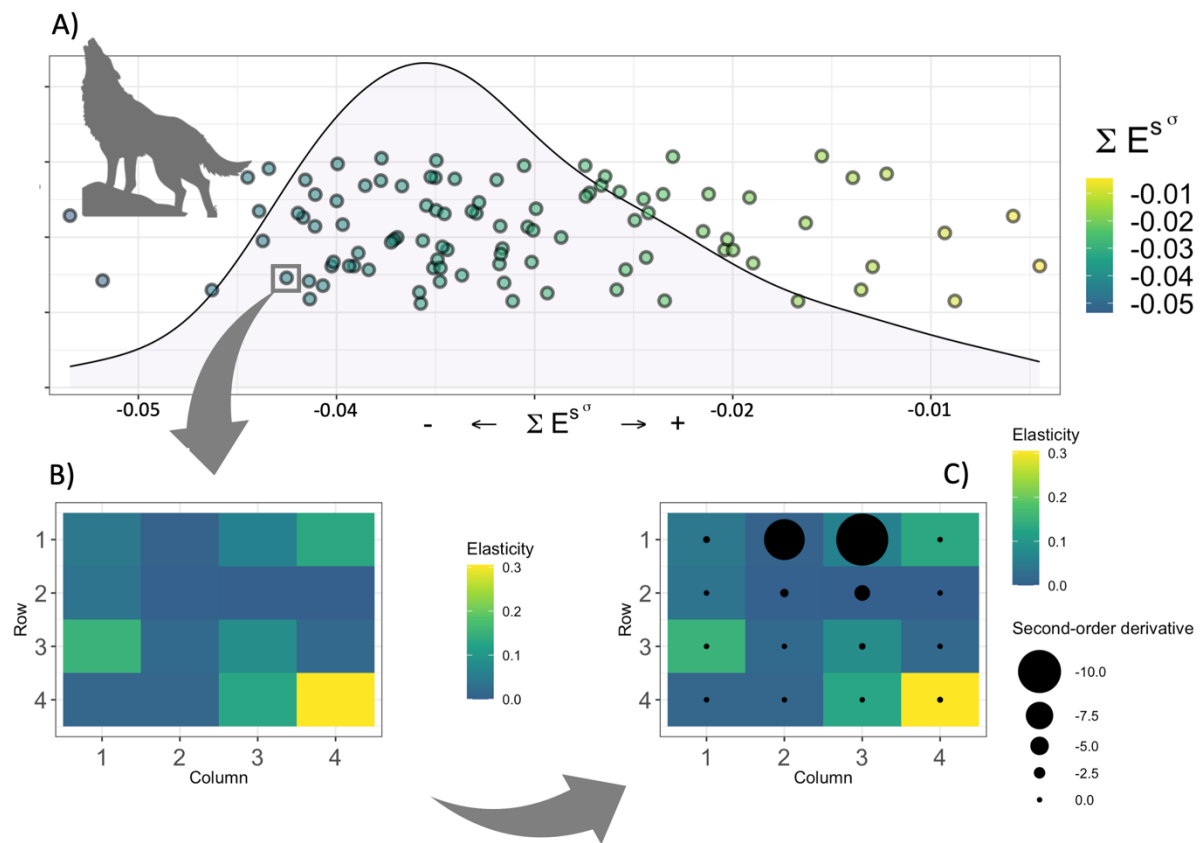
- Griffith, A.B. (2017). Perturbation approaches for integral projection models. *Oikos*, 126, 1675–1686.
- Haridas, C. V. & Tuljapurkar, S. (2005). Elasticities in Variable Environments: Properties and Implications. *Am Nat*, 166, 481–495.
- Healy, K., Ezard, T.H.G., Jones, O.R., Salguero-Gómez, R. & Buckley, Y.M. (2019). Animal life history is shaped by the pace of life and the distribution of age-specific mortality and reproduction. *Nat Ecol Evol*, 3, 1217–1224.
- Heppell, S.S. (1998). Application of Life-History Theory and Population Model Analysis to Turtle Conservation. *Copeia*, 1998, 367.
- Hilde, C.H., Gamelon, M., Sæther, B.-E., Gaillard, J.-M., Yoccoz, N.G. & Pélabon, C. (2020). The Demographic Buffering Hypothesis: Evidence and Challenges. *Trends Ecol Evol*, 35, 523–538.
- Jäkäläniemi, A., Ramula, S. & Tuomi, J. (2013). Variability of important vital rates challenges the demographic buffering hypothesis. *Evol Ecol*, 27, 533–545.
- Jones, J.H. (2007). demogR: A Package for the Construction and Analysis of Age-structured Demographic Models in R. *J Stat Softw*, 22, 1–28.
- Jones, J.H. (2011). Primates and the evolution of long, slow life histories. *Current Biology*, 21, R708–R717.
- Jongejans, E., De Kroon, H., Tuljapurkar, S. & Shea, K. (2010). Plant populations track rather than buffer climate fluctuations. *Ecol Lett*, 13, 736–743.
- Kajin, M., Gentile, R., Almeida, P.J.A.L. de, Vieira, M.V. & Cerqueira, R. (2023). Vital rates, their variation and natural selection: a case for an Atlantic forest marsupial. *Oecologia Australis*, 27.
- Kendall, B.E., Fujiwara, M., Diaz-Lopez, J., Schneider, S., Voigt, J. & Wiesner, S. (2019). Persistent problems in the construction of matrix population models. *Ecol Modell*, 406, 33–43.
- Keyfitz, N. & Flieger, W. (1990). *World Population Growth and Aging: Demographic Trends in the Late Twentieth Century*. University of Chicago Press, Chicago.
- Koons, D.N., Pavard, S., Baudisch, A. & Jessica E. Metcalf, C. (2009). Is life-history buffering or lability adaptive in stochastic environments? *Oikos*, 118, 972–980.
- Kroon, H. De, Groenendaal, J. Van & Ehrlen, J. (2000). Elasticities: A review of methods and model limitations. *Ecology*, 81, 607–618.
- de Kroon, H., Plaisier, A., van Groenendaal, J. & Caswell, H. (1986). Elasticity: The Relative Contribution of Demographic Parameters to Population Growth Rate. *Ecology*, 67, 1427–1431.
- Lawler, R.R., Caswell, H., Richard, A.F., Ratsirarson, J., Dewar, R.E. & Schwartz, M. (2009). Demography of Verreaux’s sifaka in a stochastic rainfall environment. *Oecologia*, 161, 491–504.
- Lefèvre, C.D., Nash, K.L., González-Cabello, A. & Bellwood, D.R. (2016). Consequences of extreme life history traits on population persistence: do short-lived gobies face demographic bottlenecks? *Coral Reefs*, 35, 399–409.
- McDonald, J.L., Franco, M., Townley, S., Ezard, T.H.G., Jelbert, K. & Hodgson, D.J. (2017). Divergent demographic strategies of plants in variable environments. *Nat Ecol Evol*, 1, 0029.
- Morris, W.F., Altmann, J., Brockman, D.K., Cords, M., Fedigan, L.M., Pusey, A.E., *et al.* (2011). Low Demographic Variability in Wild Primate Populations: Fitness Impacts of Variation, Covariation, and Serial Correlation in Vital Rates. *Am Nat*, 177, E14–E28.
- Morris, W.F. & Doak, D.F. (2004). Buffering of Life Histories against Environmental Stochasticity: Accounting for a Spurious Correlation between the Variabilities of Vital Rates and Their Contributions to Fitness. *Am Nat*, 163, 579–590.

- Morris, W.F., Pfister, C.A., Tuljapurkar, S., Haridas, C. V., Boggs, C.L., Boyce, M.S., *et al.* (2008). Longevity can buffer plant and animal populations against changing climatic variability. *Ecology*, 89, 19–25.
- Münkemüller, T., Lavergne, S., Bzeznik, B., Dray, S., Jombart, T., Schiffrers, K., *et al.* (2012). How to measure and test phylogenetic signal. *Methods Ecol Evol*, 3, 743–756.
- Pélabon, C., Hilde, C.H., Einum, S. & Gamelon, M. (2020). On the use of the coefficient of variation to quantify and compare trait variation. *Evol Lett*, 4, 180–188.
- Perret, D.L., Evans, M.E.K. & Sax, D.F. (2024). A species' response to spatial climatic variation does not predict its response to climate change. *Proc Natl Acad Sci U S A*, 121, e2304404120.
- Pfister, C. (1998). Patterns of variance in stage-structured populations: Evolutionary predictions and ecological implications. *Proceedings of the National Academy of Sciences*, 95, 213–218.
- R Core Team. (2024). R: A Language and Environment for Statistical Computing.
- Reed, A.W. & Slade, N.A. (2012). Buffering and plasticity in vital rates of oldfield rodents. *Journal of Animal Ecology*, 81, 953–959.
- Rodríguez-Caro, R.C., Capdevila, P., Graciá, E., Barbosa, J.M., Giménez, A. & Salguero-Gómez, R. (2021). The limits of demographic buffering in coping with environmental variation. *Oikos*, 130, 1346–1358.
- Römer, G., Dahlgren, J.P., Salguero-Gómez, R., Stott, I.M. & Jones, O.R. (2024). Plant demographic knowledge is biased towards short-term studies of temperate-region herbaceous perennials. *Oikos*, 2024.
- Rotella, J.J., Link, W.A., Chambert, T., Stauffer, G.E. & Garrott, R.A. (2012). Evaluating the demographic buffering hypothesis with vital rates estimated for Weddell seals from 30 years of mark-recapture data. *Journal of Animal Ecology*, 81, 162–173.
- Salguero-Gómez, R. (2021). Commentary on the life history special issue: The fast-slow continuum is not the end-game of life history evolution, human or otherwise. *Evolution and Human Behavior*, 42, 281–283.
- Salguero-Gómez, R. (2024). More social species live longer, have higher generation times, and longer reproductive windows. *bioRxiv*; <https://doi.org/10.1101/2024.01.22.575897>.
- Salguero-Gómez, R., Jackson, J. & Gascoigne, S.J.L. (2021). Four key challenges in the open-data revolution. *Journal of Animal Ecology*, 90, 2000–2004.
- Salguero-Gómez, R., Jones, O.R., Archer, C.R., Bein, C., de Buhr, H., Farack, C., *et al.* (2016). COMADRE: A global data base of animal demography. *Journal of Animal Ecology*, 85, 371–384.
- Sanghvi, K., Vega-Trejo, R., Nakagawa, S., Gascoigne, S.J.L., Johnson, S.L., Salguero-Gómez, R., *et al.* (2024). Meta-analysis shows no consistent evidence for senescence in ejaculate traits across animals. *Nat Commun*, 15, 558.
- Shyu, E. & Caswell, H. (2014). Calculating second derivatives of population growth rates for ecology and evolution. *Methods Ecol Evol*, 5, 473–482.
- Simmonds, E.G. & Jones, O.R. (2024). Uncertainty propagation in matrix population models: Gaps, importance and guidelines. *Methods Ecol Evol*, 15, 427–438.
- Stearns, S. (1992). *The Evolution of Life Histories*. Oxford University Press, New York, USA.
- Stearns, S.C. (1983). The Influence of Size and Phylogeny on Patterns of Covariation among Life-History Traits in the Mammals. *Oikos*, 41, 173.
- Stubben, C., Milligan, B., Nantel, P. & Stubben, M.C. (2020). Package 'popbio.'
- Sutherland, W.J., Freckleton, R.P., Godfray, H.C.J., Beissinger, S.R., Benton, T., Cameron, D.D., *et al.* (2013). Identification of 100 fundamental ecological questions. *Journal of Ecology*, 101, 58–67.

- Tuljapurkar, S. (1990). Population Dynamics in Variable Environments. In: *Lecture notes in Biomathematics*, Lecture Notes in Biomathematics (ed. Levin, S.). Springer Berlin Heidelberg.
- Tuljapurkar, S. (2010). Environmental variance, population growth and evolution. *J Anim Ecol*, 79, 1–3.
- Tuljapurkar, S., Gaillard, J.-M. & Coulson, T. (2009). From stochastic environments to life histories and back. *Philosophical Transactions of the Royal Society B: Biological Sciences*, 364, 1499–1509.
- Tuljapurkar, S., Horvitz, C.C. & Pascarella, J.B. (2003). The Many Growth Rates and Elasticities of Populations in Random Environments. *Am Nat*, 162, 489–502.
- Tuljapurkar, S., Jaggi, H., Gascoigne, S.J.L., Zuo, W., Kajin, M. & Salguero-Gómez, R. (2023). From disturbances to nonlinear fitness and back. *bioRxiv*, 2023.10.20.563360.
- Tuljapurkar, S.D. (1982). Population dynamics in variable environments. III. Evolutionary dynamics of r-selection. *Theor Popul Biol*, 21, 141–165.
- Vázquez, D.P., Gianoli, E., Morris, W.F. & Bozinovic, F. (2017). Ecological and evolutionary impacts of changing climatic variability. *Biological Reviews*, 92, 22–42.
- Wang, J., Yang, X., Silva Santos, G., Ning, H., Li, T., Zhao, W., *et al.* (2023). Flexible demographic strategies promote the population persistence of a pioneer conifer tree (*Pinus massoniana*) in ecological restoration. *For Ecol Manage*, 529, 120727.
- Zuidema, P.A. & Franco, M. (2001). Integrating vital rate variability into perturbation analysis: an evaluation for matrix population models of six plant species. *Journal of Ecology*, 89, 995–1005.

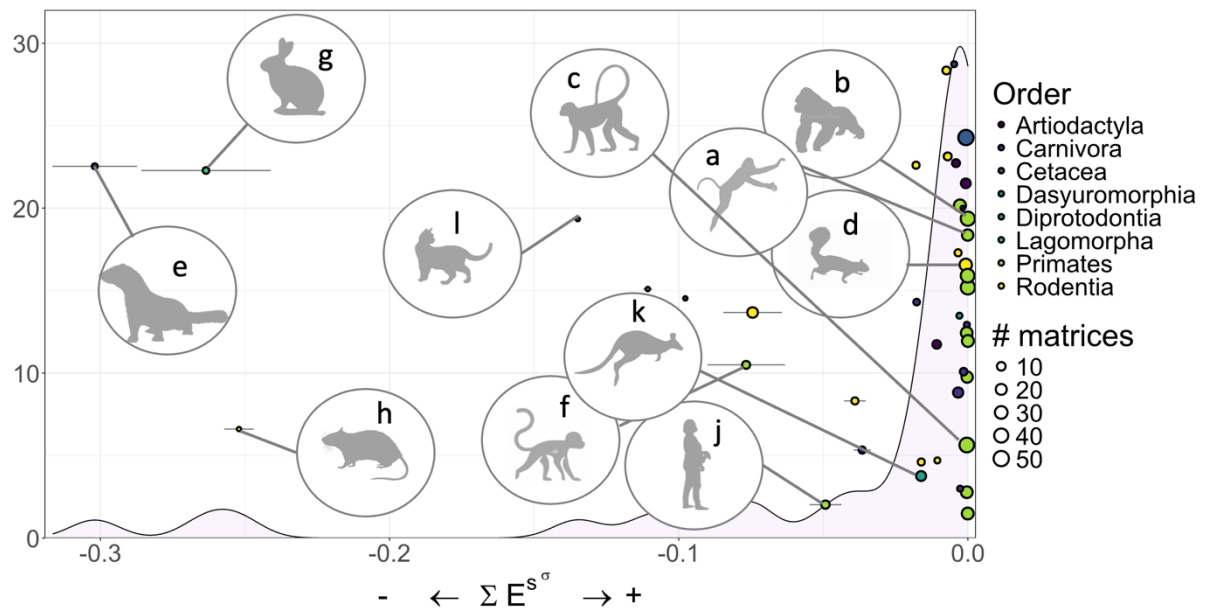


701 **Figure 1**



702

703 **Figure 2**



704  
705

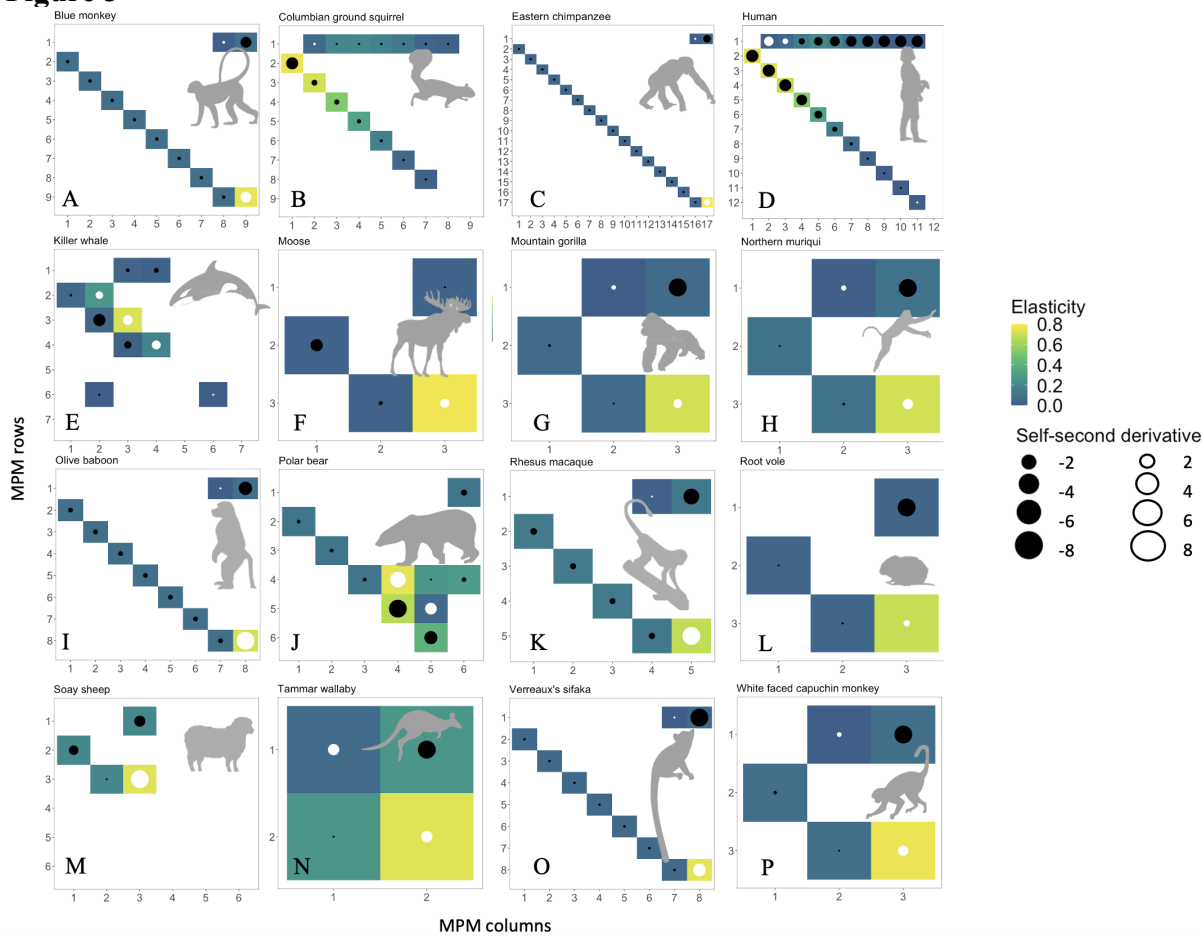


## Figure legends

**Figure 1.** A) The variance continuum for 37 hypothetical species based on the summed stochastic elasticities ( $\Sigma E_{a_{ij}}^{S\sigma}$ ) at the between populations hierarchical level. The closer the  $\Sigma E_{a_{ij}}^{S\sigma}$  is to zero, the weaker the impact of variation in demographic processes on the stochastic population growth rate,  $\lambda_s$ . The variance continuum ranges from potentially buffered (right-hand side) to less buffered (left-hand side) species/populations. The yellow-dotted species/populations can be classified as having potentially *buffered life cycles*. The left-hand side of the graph represents species/populations where variability in demographic processes results in strong impact on  $\lambda_s$  (blue dots). Thus, the blue-dotted species/populations can be classified as having potentially *unbuffered life cycles*. The vertical axis delineates the values of the probability density function, indicating the number of species/populations at each value of  $\Sigma E_{a_{ij}}^{S\sigma}$ . The placement of data points (species/populations) along the horizontal axis corresponds to their calculated values of  $\Sigma E_{a_{ij}}^{S\sigma}$  and is arranged linearly, while the placement along the y-axis is random for improved visual comprehension. B) First-order effects or linear selection pressures for individual species/populations at within-species level (see text). Shown are the elasticities of the deterministic population growth rate ( $\lambda_l$ ) for a hypothetical population of wolves and revealing the governing demographic process(es) in the life cycle (yellow cells: high elasticity, blue cells: low elasticity). C) Combined results for first (yellow and blue cells) and second order effects (black dots), where the latter reveals the nonlinear selection pressures at the within-species level.

**Figure 2.** The variance continuum for 43 populations from 37 species of mammals from the COMADRE database based on the summed stochastic elasticities ( $\Sigma E_{a_{ij}}^{S\sigma}$ ) at the between populations hierarchical level. Colors represent different taxonomic orders with Primates occupying the right-hand side. Silhouettes: a) *Brachyteles hyphoxantus*, b) *Gorilla beringhei*,

c) *Cercopithecus mitis*, d) *Urocyon v. columbianus*, e) *Mustela erminea*, f) *Erythrocebus*  
 patas, g) *Lepus americanus*, h) *Rattus fuscipes*, i) *Ovis aries*, j) *Homo sapiens*, k) *Macropus*  
*eugenii*, and l) *Felis catus*. The vertical axis delineates the values of the probability density  
 function, indicating the number of species/populations at each value of  $\Sigma E_{a_{ij}}^{S\sigma}$ . The placement  
 of data points (species/populations) along the horizontal axis corresponds to their calculated  
 values of  $\Sigma E_{a_{ij}}^{S\sigma}$  and is arranged linearly, while the placement along the y-axis is random for  
 improved visual comprehension.

**Figure 3:** First- and second-order effects on population growth rate,  $\lambda_I$  (corresponding to  
 elasticities and self-second derivatives of population growth rate, respectively) for 16  
 mammal species. The 16 plots represent populations where the MPMs built by ages were  
 available in the COMADRE Animal Matrix Database. The yellow-blue colour scale  
 represents elasticity values for each of the demographic processes in the MPM, where yellow  
 cells represent high and blue cells low elasticity of population growth rate to changes in  
 demographic processes. No colour means elasticity=0. The black dots represent negative self-  
 second derivatives of  $\lambda_I$  - corresponding to concave selection - and the white dots represent  
 positive self-second derivatives of  $\lambda_I$  - ditto convex selection. The dot sizes are scaled by the  
 absolute value of self-second derivatives, where the smaller the dot, the closer a self-second  
 derivative is to 0, indicating weak or no nonlinearity. Thus, large dots indicate strong  
 nonlinear selection forces, either concave (black) or convex (white). Since the derivatives of  
 population growth rate are confounded by eigen-structure (Kroon *et al.* 2000), the scaling of  
 the elasticity values and second-derivative values is species specific - *i.e.*, each plot has its  
 own scale. Species-specific scales can be found in Supplementary material (Table S2).

760 **Supplementary material – Data available in COMADRE Version 3.0.0 and results from Step 1 of the framework**

761

762 **Table S1.** The metadata used and the respective results presented in the main text. The first four columns represent the information from where

763 Matrix Populations Models (MPMs) were extract precisely as presented in COMADRE 3.0.0.

764

Species	Common name	Species (COMADRE)	Order	# matrices	$\lambda_l$	$\lambda_s$	$\Sigma E_{a_{ij}}^{s\sigma}$	$\Sigma E_{a_{ij}}^{s\sigma}(\text{SE})$
<i>Homo sapiens sapiens</i>	Human	Homo_sapiens_sub sp._sapiens	Primates	26	1.063707	1.061537	-2.24E-03	3.15E-04
<i>Alces alces</i>	Moose	Alces_alces	Artiodactyla	14	1.205368	1.205161	-6.69E-04	8.42E-05
<i>Antechinus agilis</i>	Agile antechinus	Antechinus_agilis	Dasyuromorphia	3	0.931076	0.885919	-1.11E-01	1.62E-03
<i>Bos primigenius</i>	Cattle	Bos_primigenius	Artiodactyla	8	1.002505	1.000493	-2.83E-03	2.96E-04
<i>Brachyteles hypoxanthus</i>	Northern muriqui	Brachyteles_hypoxanthus	Primates	25	1.05122	1.051273	-5.31E-05	2.09E-05
<i>Callospermophilus lateralis</i>	Golden-mantled ground squirrel	Callospermophilus_lateralis	Rodentia	18	2.052345	1.970253	-6.68E-02	8.72E-03
<i>Cebus capucinus</i>	White faced capuchin monkey	Cebus_capucinus	Primates	22	1.020887	1.020868	-2.04E-04	4.75E-05
<i>Cercopithecus mitis</i>	Blue monkey	Cercopithecus_mitis	Primates	28	1.036082	1.036075	-4.43E-05	1.18E-05

Cervus canadensis subsp. nelsoni	Rocky Mountain elk	Cervus_canadensis_subsp._nelsoni	Artiodactyla	10	1.107412	1.099838	-8.55E-03	1.09E-03
Eumetopias jubatus	Northern sea lion; Steller sea lion	Eumetopias_jubatus	Carnivora	4	0.904383	0.902155	-4.52E-03	2.44E-04
Felis catus	Feral cat	Felis_catus	Carnivora	3	1.948471	1.8259	-1.34E-01	1.89E-03
Gorilla beringei	Mountain gorilla	Gorilla_beringei	Primates	41	1.026827	1.02682	-1.28E-05	1.32E-05
Hippocamelus bisulcus	Huemul deer	Hippocamelus_bisulcus	Artiodactyla	3	0.996197	0.995462	-1.80E-03	1.09E-04
Leopardus pardalis	Ocelot	Leopardus_pardalis	Carnivora	4	1.086146	1.086122	-2.94E-04	3.89E-05
Lepus americanus	Snowshoe hare	Lepus_americanus	Lagomorpha	5	0.811904	0.707678	-2.62E-01	2.33E-02
Lycaon pictus	African wild dog	Lycaon_pictus	Carnivora	3	1.500429	1.430517	-9.70E-02	9.91E-04
Macaca mulatta	Rhesus macaque	Macaca_mulatta_3	Primates	24	1.127496	1.12735	-3.84E-04	6.83E-05
Macropus eugenii	Tammar wallaby	Macropus_eugenii	Diprotodontia	15	0.981097	0.970794	-1.43E-02	1.62E-03
Marmota flaviventris	Yellow-bellied marmot	Marmota_flaviventris_2	Rodentia	8	0.89031	0.886098	-8.80E-03	6.98E-04
Marmota flaviventris	Yellow-bellied marmot	Marmota_flaviventris_3	Rodentia	8	0.920541	0.916392	-7.00E-03	7.04E-04

Microtus oeconomus	Root vole	Microtus_oeconomus	Rodentia	28	1.027531	1.027095	-5.60E-04	1.06E-04
Mustela erminea	Stoat	Mustela_erminea	Carnivora	4	1.258462	1.074391	-3.10E-01	1.62E-02
Orcinus orca	Killer whale	Orcinus_orca_2	Cetacea	50	0.998658	0.998351	-4.72E-04	1.53E-04
Ovis aries	Soay sheep	Ovis_aries_2	Artiodactyla	6	1.09877	1.080656	-3.45E-02	2.96E-03
Pan troglodytes subsp. schweinfurthii	Eastern chimpanzee	Pan_troglodytes_subsp._schweinfurthii	Primates	45	0.982286	0.982191	-1.94E-04	5.06E-05
Papio cynocephalus	Olive baboon	Papio_cynocephalus	Primates	37	1.053872	1.053789	-2.41E-04	6.97E-05
Peromyscus maniculatus	Deer mouse	Peromyscus_maniculatus_2	Rodentia	4	1.10686	1.101117	-9.41E-03	6.88E-04
Phascolarctos cinereus	Koala	Phascolarctos_cinereus_2	Diprotodontia	4	1.064011	1.062744	-2.53E-03	2.16E-04
Phocarctos hookeri	New Zealand sea lion	Phocarctos_hookeri	Carnivora	16	1.023016	1.020083	-3.56E-03	4.15E-04
Propithecus verreauxi	Verreaux's sifaka	Propithecus_verreauxi	Primates	24	0.985592	0.985399	-3.06E-04	6.29E-05
Rattus fuscipes	Bush rat	Rattus_fuscipes	Rodentia	3	1.304662	1.188931	-2.45E-01	4.29E-03
Urocitellus armatus	Uinta ground squirrel	Spermophilus_armatus	Rodentia	6	1.125011	1.113416	-1.73E-02	1.68E-03



Urocitellus armatus	Uinta ground squirrel	Spermophilus_armatus_2	Rodentia	6	1.094693	1.084304	-1.47E-02	1.56E-03
Urocitellus columbianus	Columbian ground squirrel	Spermophilus_columbianus	Rodentia	6	1.008949	0.984575	-3.80E-02	3.26E-03
Urocitellus columbianus	Columbian ground squirrel	Spermophilus_columbianus_3	Rodentia	6	1.200353	1.197473	-3.38E-03	6.96E-04
Ursus americanus subsp. floridanus	Florida black bear	Ursus_americanus_subsp._floridanus	Carnivora	4	1.01989	1.018094	-3.68E-03	3.97E-04
Ursus arctos subsp. horribilis	Grizzly bear	Ursus_arctos_subsp._horribilis_5	Carnivora	7	1.025712	1.024785	-1.38E-03	1.26E-04
Ursus maritimus	Polar bear	Ursus_maritimus_2	Carnivora	5	0.940646	0.931697	-1.91E-02	9.23E-04
Brachyteles hypoxanthus	Northern muriqui	Brachyteles_hypoxanthus_2	Primates	25	1.110953	1.110983	1.22E-05	5.05E-06
Cebus capucinus	White-faced capuchin monkey	Cebus_capucinus_2	Primates	22	1.059311	1.059248	-1.03E-04	2.85E-05
Chlorocebus aethiops	Vervet	Chlorocebus_aethiops_2	Primates	8	1.187136	1.148862	-8.03E-02	1.31E-02
Erythrocebus patas	Patas monkey	Erythrocebus_patas	Primates	9	1.127974	1.092178	-5.21E-02	5.38E-03
Gorilla beringei subsp. beringei	Mountain gorilla	Gorilla_beringei_subsp._beringei	Primates	41	1.052588	1.05255	-6.81E-05	1.11E-05

**Table S2.** The species-specific scales for the elasticity of  $\lambda_I$  to changes in demographic processes and for the self-second derivatives of  $\lambda_I$  with respect to demographic processes for the 16 mammal species studied.

Figure 3 reference	Species common name	$E_{\min}$ =elasticity minimum value	$E_{\max}$ =elasticity maximum value	$SSD_{\min}$ =self-second derivative minimum value	$SSD_{\max}$ =self-second derivative maximum value
A	Blue monkey	0	0.52	-1.25	1.27
B	Columbian ground squirrel	0	0.23	-1.48	0.01
C	Eastern chimpanzee	0	0.60	-4.39	2.59
D	Human	0	0.18	-0.15	0.08
E	Killer whale	0	0.55	-5.72	3.43
F	Moose	0	0.55	-0.66	0.36
G	Mountain gorilla	0	0.81	-1.46	0.28
H	Northern muriqui	0	0.72	-1.17	0.35
I	Olive baboon	0	0.54	-0.57	1.13
J	Polar bear	0	0.26	-0.73	0.54
K	Rhesus macaque	0	0.51	-0.54	0.71
L	Root vole	0	0.86	-2.54	0.22
M	Soay sheep	0	0.56	-0.22	0.40
N	Tammar wallaby	0	0.55	-0.64	0.34
O	Verreaux's sifaka	0	0.60	-2.64	1.34
P	White faced capuchin monkey	0	0.66	-2.66	1.21